

Fallback onto Kicked Neutron Stars and its Effect on Spin-Kick Alignment

Bernhard Müller^{1,2}★

¹*School of Physics and Astronomy, Monash University, VIC 3800, Australia*

²*ARC Centre of Excellence for Gravitational Wave Discovery – OzGrav*

28 September 2023

ABSTRACT

Fallback in core-collapse supernova explosions is potentially of significant importance for the birth spins of neutron stars and black holes. It has recently been pointed out that the angular momentum imparted onto a compact remnant by fallback material is subtly intertwined with its kick because fallback onto a moving neutron star or black hole will preferentially come from a conical region around its direction of travel. We show that contrary to earlier expectations such one-sided fallback accretion onto a neutron star will tend to produce spin-kick misalignment. Since the baroclinic driving term in the vorticity equation is perpendicular to the nearly radial pressure gradient, convective eddies in the progenitor as well as Rayleigh-Taylor plumes growing during the explosion primarily carry angular momentum perpendicular to the radial direction. Fallback material from the accretion volume of a moving neutron star therefore carries substantial angular momentum perpendicular to the kick velocity. We estimate the seed angular momentum fluctuations from convective motions in core-collapse supernova progenitors and argue that accreted fallback material will almost invariably be accreted with the maximum permissible specific angular momentum for reaching the Alfvén radius. This imposes a limit of $\sim 10^{-2} M_{\odot}$ of fallback accretion for fast-spinning young neutron stars with periods of ~ 20 ms and less for longer birth spin periods.

Key words: supernovae: general — stars: neutron — hydrodynamics

1 INTRODUCTION

One of the key challenges in the theory of core-collapse supernova explosions of massive stars is to explain the birth properties of neutron stars and black holes. Phenomenological supernova models (Ugliano et al. 2012; Sukhbold et al. 2016; Müller et al. 2016a; Ebinger et al. 2019; Ertl et al. 2020) and multi-dimensional simulations (for recent reviews, see Müller 2020; Burrows & Vartanyan 2021) have already shed considerable light on the stellar progenitor properties that determine whether the collapse results in neutron star or black hole formation, and on the birth mass distribution of compact objects. The theoretical understanding of neutron star birth velocities (kicks) now appears very mature as well and points to the “gravitational tugboat mechanism” in asymmetric explosions as a natural way to account for neutron star kicks of several 100 km s^{-1} and up to $\gtrsim 1000 \text{ km s}^{-1}$ (Scheck et al. 2006; Wongwathanarat et al. 2010, 2013; Müller et al. 2017, 2019; Bollig et al. 2021; Coleman & Burrows 2022) as observed in nature, although asymmetric neutrino emission (Stockinger et al. 2020; Coleman & Burrows 2022) will also play a – probably subdominant – role, and other, more hypothetical kick mechanisms are conceivable. It has also been realised that the tugboat mechanism may produce black holes with kicks in “fallback explosions” with partial mass ejection (Janka 2013; Chan et al. 2018, 2020), in line with observational evidence.

The origin of neutron star spins remains more elusive for several reasons. On the one hand, it is far from clear to what extent the spins are determined by the angular momentum of the progenitor

core, or rather by spin-up and spin-down processes during the explosion. Recent multi-dimensional simulations suggest that spin-up by asymmetric accretion could be the dominant mechanism for setting neutron star birth spins and might produce a realistic range of birth spin rates from a few seconds down to ~ 10 s as in the observed pulsar population (Popov & Turolla 2012; Igoshev & Popov 2013; Noutsos et al. 2013). However, our incomplete knowledge of the interior rotation rates of massive stars (Heger et al. 2000, 2005; Langer 2012; Fuller et al. 2019) and uncertainties about early spin-down processes mediated by magnetic fields make it difficult to draw firm conclusions.

Among compact object birth properties, perhaps the greatest challenge to current core-collapse supernova models consists in strong observational evidence that neutron star spins and kicks tend to be aligned (Kramer et al. 2003; Johnston et al. 2005; Noutsos et al. 2012, 2013; Yao et al. 2021). Several mechanisms for spin-kick alignment have been proposed over the years; some of these are purely hydrodynamic in nature, while others invoke kicks generated by asymmetric emission of neutrinos or radiation from very strongly magnetised neutron stars (e.g., Harrison & Tademaru 1975; Spruit & Phinney 1998; Arras & Lai 1999; Lai et al. 2001; Socrates et al. 2005; Wang et al. 2007; Fragione & Loeb 2023). Multi-dimensional simulations have rather stubbornly refused to bear out any of the suggested hydrodynamic mechanisms and cannot yet reproduce systematic spin-kick alignment (Wongwathanarat et al. 2013; Powell & Müller 2019, 2020; Janka et al. 2022; Powell et al. 2023). Some recent three-dimensional models by Coleman & Burrows (2022) show strong spin-kick alignment or anti-alignment, but the majority of their models still exhibit large angles between the spin and kick direction.

★ E-mail: bernhard.mueller@monash.edu

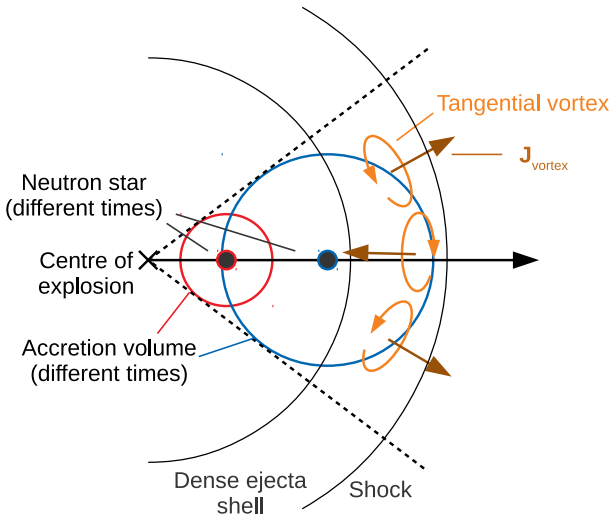


Figure 1. Simplified sketch of one-sided neutron star fallback accretion as outlined by [Janka et al. \(2022\)](#). As the neutron star moves away from the centre of explosion, so does the spherical accretion volume (red and blue circles), tracing out a conical region within the ejecta from which fallback material may be supplied. The ejecta are compressed into a dense shell behind the shock (outer black circle). [Janka et al. \(2022\)](#) posit that vortices originating from convective motions in the progenitor star are “flattened” as they are run over and radially compressed by the shock so that their vorticity and angular momentum vectors $\mathbf{J}_{\text{vortex}}$ predominantly point radially outward or inward.

For this reason, [Janka et al. \(2022\)](#) argued that spin-kick alignment could be due to fallback on longer time scales than the first ~ 1 s that can presently be studied by rigorous three-dimensional simulations. They note that the neutron star will preferentially accrete fallback material along its direction of motion, and argue that stochastic vortical motions in the accreted material, ultimately arising from convective eddies in the outer shells, will then tend to magnify the neutron star angular momentum component along its direction of motion (Figure 1). Interestingly, the proposed mechanism does not require any progenitor rotation. The dynamical impact of angular momentum fluctuations from convective regions in fallback supernovae is also of broader interest because since it could lead to disk formation during the infall and power late-time outflows ([Gilkis & Soker 2014](#); [Antoni & Quataert 2022, 2023](#); [Soker 2023](#)).

In this paper, we shall revisit this idea and argue that this mechanism is more likely to destroy spin-kick alignment than to facilitate it if the interaction of the supernova shock wave with convective eddies in the progenitor is examined more closely. If true this gives a different twist to the original idea of [Janka et al. \(2022\)](#). However, as the phenomenon of one-sided accretion pointed out by [Janka et al. \(2022\)](#) is likely a robust feature of fallback explosion, their idea can then be used to place constraints on the amount of fallback in supernova explosions. Based on the typical convective velocities in supernova progenitors and physical constraints on the accretion process, we shall discuss implications for the permitted amount of fallback in typical core-collapse supernovae.

2 SUMMARY OF MODEL FOR SPIN-KICK ALIGNMENT

It is useful to first review the geometrical picture for fallback on a moving neutron star outlined by [Janka et al. \(2022\)](#). Their proposed

scenario is sketched in Figure 1. [Janka et al. \(2022\)](#) point out that fallback is likely to affect ejecta that move with sufficiently small velocity v with respect to a neutron star of mass M for their kinetic energy to be of the same order to their potential energy or smaller. This defines the maximum distance of prospective fallback material to the neutron star R_{acc} ([Shapiro & Teukolsky 1983](#)) (accretion radius),

$$\xi \frac{GM}{R_{\text{acc}}} = \frac{1}{2}v^2, \quad (1)$$

with a non-dimensional factor ξ of order unity. [Janka et al. \(2022\)](#) then demonstrate that for a homologously expanding explosion and a few further assumptions, the volume defined by Equation (1) is indeed roughly spherical and centred around the current location of the neutron star, and that the distance of the neutron star from the geometric centre of the explosion will easily be comparable to or larger than R_{acc} . This implies very asymmetric accretion by the neutron star, mostly from ahead of its direction of travel, where the accretion volume reaches furthest (or is most likely to reach) into the shell of dense, shock-compressed ejecta.

For such asymmetric fallback of material forward of the neutron star to lead to spin-kick alignment, [Janka et al. \(2022\)](#) make the crucial assumption that vortex motions in the fallback material primarily occur perpendicular to the radial direction such that the vorticity ω and specific angular momentum \mathbf{j} of the accreted material has a dominant *radial* component. Under the assumption of [Janka et al. \(2022\)](#) that the radial ejecta velocities v_r are perfectly spherically symmetric, that only non-radial (transverse) velocity perturbations \mathbf{v}_t are present in the ejecta, and that no further exchange of angular momentum occurs during fallback, the angular momentum of accreted vortices is simply

$$\mathbf{J} = \int \rho \mathbf{r} \times \delta \mathbf{v}_t dV, \quad (2)$$

where the integral extends over the fallback region.¹ Even if the neutron star may accrete vortices with a stochastically varying sense of circulation, the net effect will be to add a large amount of angular momentum with a direction close to the neutron star displacement vector \mathbf{D}_{NS} from the centre of explosion and the neutron star velocity \mathbf{v}_{NS} . If the angular momentum added by fallback is larger in terms of magnitude than the initial neutron star angular momentum, this would drive the neutron star towards spin-kick alignment.

The critical question for this mechanism is whether the specific angular momentum of vortices in the compressed ejecta shell indeed tends to be aligned with the radial direction. There are two possible (and interrelated) scenarios for the formation of such vortices. The vortices may simply be relics of convective eddies from the pre-collapse stage that are compressed as they are run over by the shock ([Janka et al. 2022](#)). The desired vortices may also be generated by Rayleigh-Taylor and Richtmyer-Meshkov instabilities ([Richtmyer 1960](#); [Zhou 2017a,b](#)) that operate behind the supernova shock (e.g., [Chevalier 1976](#); [Müller et al. 1991](#); [Fryxell et al. 1991](#); [Kifonidis et al. 2006](#); [Wongwathanarat et al. 2015](#)), with the seeds of the instabilities either provided by the aforementioned eddies or initial explosion asymmetries due to convection ([Herant et al. 1992, 1994](#); [Burrows et al. 1995](#); [Janka & Müller 1995, 1996](#)) or the standing-accretion shock instability ([Blondin et al. 2003](#)) in the supernova

¹ See Section 4.2 in [Janka et al. \(2022\)](#) for a detailed discussion why other terms cancel out, and Section 4.2.3 for the case with density inhomogeneities, but still with a perfectly spherical radial velocity field $v_r(r)$.

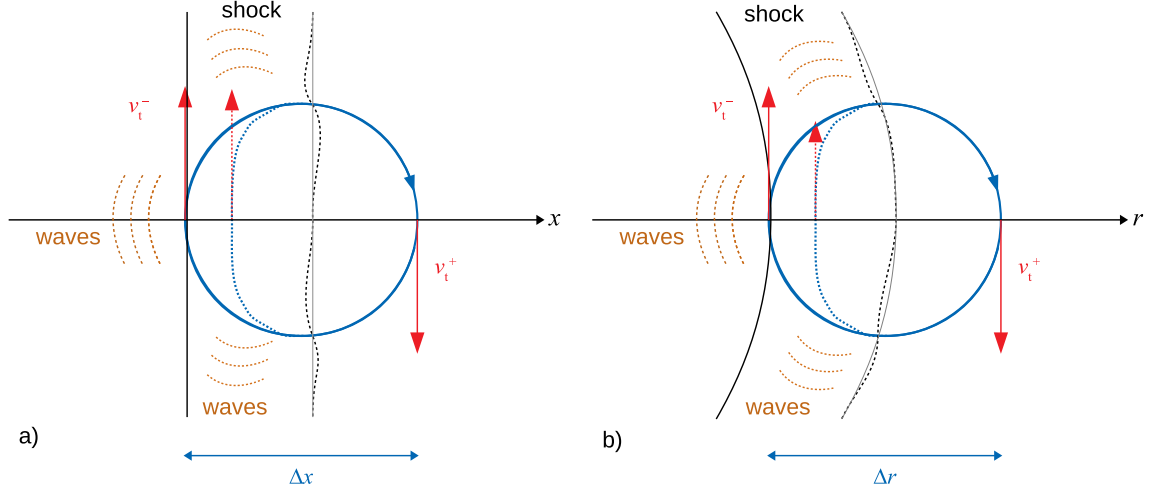


Figure 2. Interaction of a convective vortex a) with a planar shock wave and b) with a spherical shock wave. For the sake of simplicity, the pre-shock medium is assumed to have homogeneous density so that a circular flow pattern with constant velocity along the vortex fulfils the solenoidal condition for anelastic flow. The shock and the structure of the vortex are depicted at two stages, i.e., when the shock has just hit the eddy (solid lines) and when it has run further across half of the eddy (dashed lines). Red arrows indicate the transverse velocity v_t^- furthest to left (furthest inward) of the eddy and v_t^+ furthest to the right (furthest outside). The direction of shock propagation (in the x -direction and in the radial direction, respectively) and the initial extent Δx and Δr of the eddy are also shown. In the planar case v_t^- remains unchanged as the shock starts to hit the eddy and is not considerably affected later, except that waves behind the shock (orange) transport transverse momentum around to some degree. The planar shock is also slightly corrugated due to slightly inhomogeneous pre-shock conditions and wave activity downstream. In the case of a spherical shock, the picture is similar, except for one important difference. As the inner part of the eddy moves outwards after being shocked, the transverse velocity v_t^- decreases due to fictitious forces (which ensure specific angular momentum conservation). Thus the total angular momentum of the shocked eddy remains conserved despite radial compression.

core. Janka et al. (2022) argues that for strictly spherical expansion with $v_r = v_r(r)$, vortical motions in the ejecta must inevitably be purely transverse. Indeed, it may appear at first glance that “closed” vortices with transverse vorticity and angular momentum require departures from a spherically symmetric expansion law (Figure 1).

3 EVOLUTION OF VORTICES DURING THE SUPERNOVA EXPLOSION

However, these arguments do not appear conclusive and suffer from an inconsistency in the assumptions. To elucidate the issue, let us first consider the case of a convective eddy hit by the supernova shock and also make the assumption that the density and pressure fields are perfectly spherical. The eddy will be squeezed due to radial compression, but if ∇P and the gravitational acceleration \mathbf{g} are strictly radial, this implies that the specific angular momentum $\mathbf{j} = \mathbf{r} \times \mathbf{v}$ in the shocked ejecta does not change,

$$\frac{d\mathbf{j}}{dt} = -\mathbf{r} \times \frac{\nabla P}{\rho} + \mathbf{r} \times \mathbf{g} = 0, \quad (3)$$

and hence the total angular momentum in the squeezed vortex volume $V(t)$ should also be constant

$$\frac{d}{dt} \int_{V(t)} \rho \mathbf{j} dV = 0, \quad (4)$$

and identical to the angular momentum of the vortex before collapse. Without invoking non-spherical pressure perturbations, there is no mechanism for tilting eddies into a different plane and changing the direction of their angular momentum. Since convective motions in the pre-collapse phase innately involve upward and downward radial motions across the largest available scale (the width of the convection zone), and lateral flow to “close the loop” between them at the top and

bottom of the convection zone, it is intuitively clear that the angular momentum of the large-scale eddies will generally be dominated by the non-radial components. More formally, one can consider the vorticity equation,

$$\frac{d\boldsymbol{\omega}}{dt} = (\boldsymbol{\omega} \cdot \nabla)\mathbf{v} - (\boldsymbol{\omega} \cdot \nabla)\mathbf{v} - \boldsymbol{\omega}(\nabla \cdot \mathbf{v}) + \frac{\nabla\rho \times \nabla P}{\rho^2}, \quad (5)$$

and note that the baroclinic term $\nabla\rho \times \nabla P/\rho^2$ is the driving term for the vorticity evolution in convective motions² (as it corresponds to the buoyancy term as the driving term in the momentum equation). Since the non-radial components $\nabla_t \rho$ and $\nabla_t P$ of the density and pressure gradients are small compared to the radial components $\nabla_r \rho$ and $\nabla_r P$, we have

$$\frac{\nabla\rho \times \nabla P}{\rho^2} \approx \frac{\nabla_t \delta\rho \times \nabla_r P + \nabla_r \delta\rho \times \nabla_t P}{\rho^2} \perp \mathbf{r}, \quad (6)$$

i.e., for small density and pressure perturbations (as encountered in subsonic convection in supernova progenitors), buoyancy generates non-radial vorticity perturbations. Incidentally, the same argument also precludes the generation of radial vorticity by Rayleigh-Taylor instability behind the supernova shock as long as the pressure field is assumed to be spherically symmetric, as this instability also hinges on the baroclinic term (Zhou 2017a). In a nearly spherical explosion, Rayleigh-Taylor instability will again primarily generate non-radial vorticity. As long as no extreme asymmetries are assumed in the progenitor star or the supernova explosion, it appears hard to avoid the presence of vortices with *non-radial* vorticity in the shocked ejecta.

To somewhat reconcile these arguments with the intuitive notion

² Note that to effectively capture a temporally-averaged steady state of convection, one would need to perform Reynolds averaging on Equation (5)

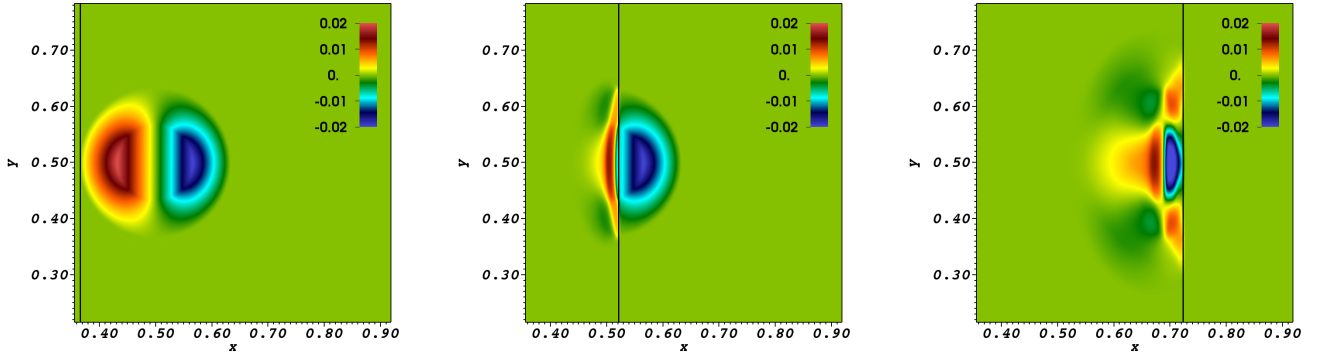


Figure 3. Transverse velocity (in dimensionless units) for a vortex overrun by a shock (black solid line) before (left panel), during (middle panel), and after the passage of the shock (right panel). The vortex is flattened to a more oblate shape, and in addition, waves that propagate sideways and downstream of the shock redistribute transverse momentum. The maximum and minimum transverse velocities before and after the passage of the shock are similar.

of “vortex flattening” by shock compression, it is useful to consider the interaction of the supernova shock with existing vortices in more depth (Figure 2). The problem of shock-vortex interaction has been studied more formally using analytic theory (Velikovich et al. 2007; Wouchuk et al. 2009) and simulations (Ellzey et al. 1995; Barbosa & Skews 2001; Zhang et al. 2005) in the case of a planar shock, and also for a stalled supernova shock during the pre-explosion phase (Huete et al. 2018), but a qualitative analysis will suffice here. If we assume the curvature of the shock is negligible over the scale of a vortex, the transverse velocity perturbations will simply be conserved across the shock. Upstream transverse velocity perturbations will leave velocity perturbations downstream of the shock, and also corrugate the shock surface. The corrugation implies that the shocked material *will* experience some change in vorticity, but while the vortex experiences some squeezing, it is not destroyed. However, the downstream perturbation will no longer be purely vortical, and acoustic waves will be produced by the shock-vortex interaction. Further coupling between vortical and acoustic perturbations will occur as the vortex expands in the wake of the shock (cp. the analogous process during the collapse phase, Abdikamalov et al. 2016; Abdikamalov & Foglizzo 2020).

To further illustrate this phenomenon, we simulate the interaction of a planar shock with a vortex in two dimensions. We set up a non-dimensional problem on a quadratic domain of size $\Delta x = \Delta y = 1$. A shock perpendicular to the x -direction is set up at $x = 0.25$ with post-shock density $\rho_p = 1.32$, pressure $P_p = 16.77$, and velocity $v_p = 8.48$ and pre-shock density $\rho_0 = 0.2$ and pressure $P_0 = 0.2$; a perfect gas with $\gamma = 4/3$ is assumed. The pre-shock medium is initially at rest except for a vortical velocity perturbation $\delta \mathbf{v} = v_{\text{rot}} = \frac{\mathbf{x} - \mathbf{x}_0}{|\mathbf{x} - \mathbf{x}_0|} \times \mathbf{e}_z$ centred around $\mathbf{x}_0 = (0.5, 0)$. The rotational velocity v_{rot} is chosen in close analogy to the Gresho vortex (Gresho & Chan 1990),

$$v_{\text{rot}} = \begin{cases} 0.3|\mathbf{x} - \mathbf{x}_0|, & |\mathbf{x} - \mathbf{x}_0| < 1/15 \\ 0.04 - 0.3|\mathbf{x} - \mathbf{x}_0| & 1/15 \leq |\mathbf{x} - \mathbf{x}_0| < 1/15 < 2/15 \\ 0, & \text{else} \end{cases} \quad (7)$$

although no pressure perturbations are imposed. The equations of compressible hydrodynamics are solved with a finite-volume code

and apply appropriate closures, but this is beyond the scope of this paper; a qualitative consideration of the driving term is sufficient for our purpose.

that employs second order reconstruction with the van Leer limiter (van Leer 1974), the HLLC Riemann solver (Toro et al. 1994) with an adaptive switch for the more dissipative HLLC solver (Einfeldt 1988) at shocks to avoid odd-even decoupling and the carbuncle phenomenon (Quirk 1994), and second-order Runge-Kutta time stepping. Transverse velocities at different stages of the shock-vortex interaction are shown in Figure 3. For this particular problem, the distortion of the shock is minimal, but deviations from the initial irrotational flow pattern are sufficient to launch waves transverse to the shock and somewhat affect the transverse velocities in the shocked eddy. However, the vortex clearly survives with transverse velocities similar to the initial conditions.

It might still appear that if the transverse velocities in a vortex are almost conserved as the vortex is shocked, the net angular momentum of the vortex could decrease simply by compression. As the total angular momentum J of the vortex is approximately

$$J = \int r \rho v_t dV \approx J \Delta M / 2 [(r + \Delta r / 2) v_t^+ + (r - \Delta r / 2) v_t^-] \\ = \Delta M / 2 \Delta r (v_t^+ + v_t^-), \quad (8)$$

in terms of the mass ΔM of the vortex, its radial extent Δr , and the transverse velocities v_t^+ and v_t^- in the outer and inner portion of the loop. Thus, if v_t^+ and v_t^- are unaffected by the shock, compression of Δr might appear to reduce J . However, it must be borne in mind that the vortex interacts with a spherical shock wave (Figure 2b). In this case, the magnitude of the transverse velocity v_t^- in the inner portion of the vortex will decrease due to fictitious forces that maintain angular momentum conservation (neglecting transverse pressure gradients) while the radial extent Δr of the vortex shrinks as the shock runs across it. If the subtle impact of fictitious forces on the transverse velocities v_t is taken into account during shock-vortex interaction, the total angular momentum of the vortex will be conserved as expected.

In summary, it seems improbable that the interaction of the supernova shock (or any reverse shocks launched later in the explosion) with convective vortices in the progenitor star, or the action of mixing instabilities behind the shock can generate vortices with nearly radial vorticity and angular momentum vectors as required for the spin-kick alignment mechanism of Janka et al. (2022). This would imply that one-sided fallback accretion in explosions of non-rotating stars destroys rather than enforces spin-kick alignment.

There is, however, one exception where eddies with radial vorticity and angular momentum could arise, namely the case of rapid

rotation. In rotating shells, a large-scale vorticity field is present, and balance between gravity, buoyancy, inertial, and pressure forces can give rise to a quasi-steady state flow structure with significant non-radial pressure variations. Due to instabilities and mode interactions, such systems often develop large-scale eddies with radial vorticity as familiar, e.g., from low-Rossby number flow in Earth’s atmosphere. The velocity fluctuations in these eddies tend to be somewhat smaller than the average rotational flow velocity. Hence, the vectorial angular momentum of fallback material will mostly be aligned with the axis of rotation, so that, as pointed out by Janka et al. (2022), fallback will still lead to spin-kick misalignment much of the time, since the neutron star kick direction appears to be selected randomly and not in alignment with the rotation axis of the progenitor according to current 3D simulations.

4 ESTIMATES FOR ANGULAR MOMENTUM DEPOSITION ON THE NEUTRON STAR

Nevertheless, the concept of one-sided accretion of Janka et al. (2022) remains important and potentially useful for constraining supernova physics. If fallback misaligns (rather than aligns) neutron star spins and kicks, this will place limits on the permissible amount of fallback in (typical) core-collapse supernovae if one can estimate the amount of angular momentum contained in accreted vortices, as we shall outline in this section.

Under the assumption that shock-vortex interaction leaves the angular momentum of shocked eddies essentially unchanged (except for some redistribution of angular momentum by waves propagating parallel to the shock surface), the accreted angular momentum can be estimated based on the convective velocities and eddy scales at the pre-collapse stage. The subsequent evolution of shocked vortices that undergo fallback is not straightforward because of vortical-acoustic coupling during the collapse phase (e.g., Kovalenko & Eremin 1998; Lai & Goldreich 2000; Abdikamalov & Foglizzo 2020) and Rayleigh-Taylor instability. However, linear theory for perturbations in the accretion flow (e.g., Kovalenko & Eremin 1998; Lai & Goldreich 2000; Abdikamalov & Foglizzo 2020) suggests that the angular momentum contained in transverse motions is approximately conserved during the infall; in the linear regime, transverse velocity perturbations asymptotically scale as $\delta v_t/v_r \propto r^{-1/2}$ (Lai & Goldreich 2000) and hence as $\delta v_t \propto r^{-1}$ for free-fall conditions. Rayleigh-Taylor instability will predominantly accelerate plumes in the radial direction and may not substantially alter the angular momentum contained in transverse velocity perturbations. With all due caveats about the full non-linear evolution of transverse velocity perturbation behind the supernova shock, it appears justified to estimate the accreted angular momentum from transverse perturbations based on pre-collapse conditions.

4.1 Upper bound for angular momentum deposited by fallback

Such estimates for the angular momentum in convective eddies at the pre-collapse stage can be based on 1D stellar evolution models implementing mixing-length theory (MLT; Biermann 1932; Böhm-Vitense 1958). MLT provides radial velocity profiles only; the transverse velocities of the biggest eddies (those that span the entire depth of a convective region) near the convective boundaries typically correspond roughly to the maxima of the radial convective velocity profiles within a convective zone (cp. Figure 10 in Müller et al. 2016b). This places an upper bound of $J \sim v_{\text{conv}} \Delta r \Delta M_{\text{eddy}}/2$ on the angular momentum of a single eddy (cp. Equation 8), which is not too different

from the estimates of Gilkis & Soker (2014). If the accreted fallback mass ΔM originates only from a portion of a pre-collapse eddy ($\Delta M < \Delta M_{\text{eddy}}$), higher values $j \sim v_{\text{conv}} R$ of the specific angular momentum of the fallback material are conceivable. In the regime $\Delta M > \Delta M_{\text{eddy}}$ the angular momentum of several pre-collapse eddies tends to cancel, and may in fact cancel more efficiently than estimated by Gilkis & Soker (2014) for eddies with uncorrelated angular momenta, but the most optimistic case with the high possible specific angular momentum will be more relevant for the subsequent discussion.

Figure 4 shows the most optimistic value $j \sim v_{\text{conv}} R$ for the specific angular momentum in pre-collapse eddies for red supergiant progenitors with $12M_{\odot}$, $15M_{\odot}$, and $18M_{\odot}$ from Müller et al. (2016a). These progenitors are fairly illustrative for the situation in red supergiants at the onset of core collapse in general. In the hydrogen shell of red supergiants, the specific angular momentum contained in transverse convective motions tends to reach large values of order $10^{18}\text{--}10^{19} \text{ cm}^2 \text{ s}^{-1}$. Even in the inner (oxygen, neon, carbon, helium) shells, the specific angular momentum in convective eddies is still appreciable ($\sim 10^{15} \text{ cm}^2 \text{ s}^{-1}$). If the specific angular momentum of fallback material were conserved during accretion onto the neutron star, even minimal amounts of fallback from the hydrogen shell could change the neutron star angular momentum appreciably and destroy any pre-existing spin-kick alignment if the neutron star accretes primarily ahead of its direction of travel. Thus, one might surmise that the unavoidable one-sided accretion pointed out by Janka et al. (2022) might actually place stringent limits on the amount of fallback matter from the hydrogen envelopes, and to a lesser extent from inner shells as well. To impart an angular momentum of $5 \times 10^{47} \text{ g cm}^2 \text{ s}^{-1}$ perpendicular to the kick direction, which is sufficient to significantly misalign a neutron star with a birth spin period of $\sim 20 \text{ ms}$ as for the Crab pulsar (Lyne et al. 2015) and a typical moment of inertia of $1.5 \times 10^{45} \text{ g cm}^2$, fallback of less than $10^{-1} M_{\odot}$ in the kick direction from an inner convective shell and of less than $10^{-4} M_{\odot}$ from the hydrogen envelope would appear sufficient.

However, avoidance of spin-kick misalignment by one-sided accretion does not actually place such stringent limits on the accreted material from the hydrogen envelope. Material with very high specific angular momentum simply cannot be accreted onto the neutron star because of centrifugal support. Unless it manages to lose angular momentum, it will instead bypass the neutron star on an orbit with a large semimajor axis, but will eventually be blown out by the neutron star wind. Less stringent upper bounds for the fallback mass ΔM may still be formulated after taking into account constraints on the specific angular momentum of accreted matter.

The worst-case misalignment can be estimated by noting that fallback material needs to reach the Alfvén radius R_A of the neutron star in order to be effectively captured and deposit its angular momentum, (provided that the Keplerian velocity at the Alfvén radius is still greater than the corotation velocity such as to avoid ejection in the propeller regime; Illarionov & Sunyaev 1975; Piro & Ott 2011). This limits its specific angular momentum to

$$j = \sqrt{2GM R_A} \quad (9)$$

for parabolic orbits. Equating the magnetic pressure (assuming a dipole field with dipole moment μ) and the ram pressure ρv^2 , R_A is determined by

$$\left(\frac{\mu}{R_A^3}\right)^2 = \frac{\dot{M} \sqrt{\frac{2GM}{R_A}}}{4\pi R_A^2}, \quad (10)$$

where \dot{M} is the accretion rate during the fallback event and the

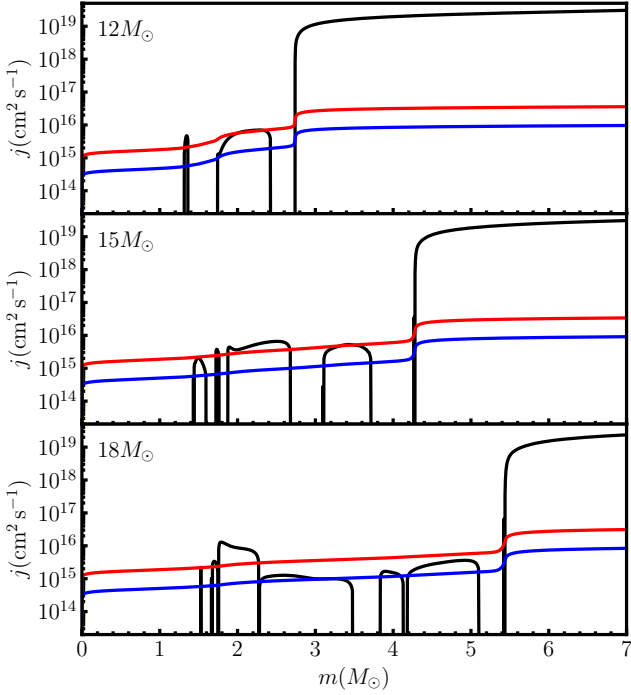


Figure 4. The typical specific angular momentum fluctuations $j = v_{\text{conv}}R$ associated with convective motions (black) and the Keplerian specific angular momentum at the Alfvén radius (Equation 13) for neutron star magnetic field strengths of 10^{12} G (blue) and 10^{14} G (red), a fallback mass of $\Delta M = 0.1M_{\odot}$, a neutron star mass of $1.4M_{\odot}$, and a neutron star radius of 12 km. Results are shown for three progenitor models with zero-age main sequence masses of $12M_{\odot}$, $15M_{\odot}$, and $18M_{\odot}$ from Müller et al. (2016a).

velocity v has been set to the escape velocity. This yields

$$R_A \sim \left(\frac{8\pi^2\mu^4}{GM^2} \right)^{1/7}, \quad (11)$$

after expressing μ in terms of the surface dipole field strength B and the neutron star radius as $\mu = BR^3$. For a rough estimate of the accretion rate during a fallback event, we can assume that fallback occurs on a free-fall time scale τ_{ff} ,

$$\tau_{\text{ff}} = \frac{\pi}{2} \left(\frac{r^3}{GM} \right)^{1/2}, \quad (12)$$

where r is the initial radial distance of the fallback blob and M is the neutron star mass. Generally, fallback will occur after material has expanded substantially from its initial radial position in the progenitor, but as the final results are not particularly sensitive to r or the timescale of fallback, the initial radial coordinate of fallback material in the progenitor provides a suitable estimate for τ_{ff} for practical purposes. Approximating the accretion rate in terms of τ_{ff} and the fallback mass ΔM as $\dot{M} \sim \Delta M/\tau_{\text{ff}}$, we find the maximum specific angular momentum of the blob,

$$\begin{aligned} j &= \frac{2^{1/14}\pi^{2/7}B^{2/7}G^{5/14}M^{5/14}r^{3/14}R^{6/7}}{\Delta M^{1/7}} \\ &= 5.2 \times 10^{15} \text{ cm}^2 \text{ s}^{-1} \times \left(\frac{B}{10^{12} \text{ G}} \right)^{2/7} \times \left(\frac{R}{12 \text{ km}} \right)^{6/7} \times \\ &\quad \left(\frac{M}{1.4M_{\odot}} \right)^{5/14} \times \left(\frac{r}{10^5 \text{ km}} \right)^{3/14} \times \left(\frac{\Delta M}{0.1M_{\odot}} \right)^{-1/7}. \end{aligned} \quad (13)$$

The maximum angular momentum ΔJ is

$$\begin{aligned} \Delta J &= 2^{1/14}\pi^{2/7}B^{2/7}G^{5/14}M^{5/14}r^{3/14}R^{6/7}\Delta M^{6/7} \\ &= 2.8 \times 10^{47} \text{ g cm}^2 \text{ s}^{-1} \times \left(\frac{B}{10^{12} \text{ G}} \right)^{2/7} \times \left(\frac{R}{12 \text{ km}} \right)^{6/7} \times \\ &\quad \left(\frac{M}{1.4M_{\odot}} \right)^{5/14} \times \left(\frac{r}{10^5 \text{ km}} \right)^{3/14} \times \left(\frac{\Delta M}{0.1M_{\odot}} \right)^{6/7}. \end{aligned} \quad (14)$$

For other purposes, it may be more useful to express ΔJ directly in terms of the duration τ of fallback accretion rather than approximating τ as the freefall time at a specific radius,

$$\begin{aligned} \Delta J &= 2^{3/14}\pi^{1/7}B^{2/7}G^{3/7}M^{3/7}R^{6/7}\Delta M^{6/7}\tau^{1/7} \\ &= 3.8 \times 10^{47} \text{ g cm}^2 \text{ s}^{-1} \times \left(\frac{B}{10^{12} \text{ G}} \right)^{2/7} \times \left(\frac{R}{12 \text{ km}} \right)^{1/7} \times \\ &\quad \left(\frac{M}{1.4M_{\odot}} \right)^{3/7} \times \left(\frac{\Delta M}{0.1M_{\odot}} \right)^{6/7} \times \left(\frac{\tau}{1 \text{ d}} \right)^{1/7}. \end{aligned} \quad (15)$$

The maximum specific angular momentum of fallback matter for $M = 1.5M_{\odot}$, $R = 12$ km, and $\Delta M = 0.1M_{\odot}$ is shown in Figure 4 for two different values of 10^{12} G and 10^{14} G for the magnetic field B for the three aforementioned progenitor models. By coincidence, the stochastic angular momentum fluctuations in the inner convective zone shells are close to the maximum sustainable specific angular momentum for fallback accretion. By contrast, fallback material from the hydrogen shell can only be accreted at considerably smaller specific angular momentum than the angular momentum fluctuations present in progenitor stars.

In practice, Equations (14,15) can therefore be used to estimate upper bounds for the angular momentum that can be imparted onto a neutron star by fallback and contribute to misalignment. ΔJ can then be compared to the typical angular momentum J of young pulsars. For the Crab pulsar with a magnetic field $4\text{--}8 \times 10^{12}$ G (Cognard et al. 1996; Lyutikov 2007; Kou & Tong 2015) and a birth spin period of ~ 20 ms (Lyne et al. 2015), and a typical moment of inertia of 1.5×10^{45} g cm², this amounts to $J \approx 5 \times 10^{47}$ g cm² s⁻¹. Substantial misalignment ($\Delta J > 0.5J$) would be achieved for fallback masses $\geq 0.01M_{\odot}$ and $R > 10^5$ km, i.e., whenever fallback is spread over at least a few minutes³. For late fallback on a timescale of $\tau = 1$ d, about $0.006M_{\odot}$ of fallback achieve the same result.

4.2 Relevance of the bound on accreted angular momentum

However, Equations (14,15) assume optimal conditions for the accreted angular momentum transverse to the kick direction. It is therefore not immediately clear that we can place limits on ΔM from our estimates for ΔJ . However, there are good arguments that the typical angular momentum of accreted fallback matter will not be too far below these optimistic estimates. In discussing how close the estimates from Equations (14,15) are to realistic fallback conditions, several factors need to be considered:

- (i) Uncertainties in the magnitude of the transverse angular momentum fluctuations of matter affected by fallback,
- (ii) Averaging effects that reduce the total angular momentum of fallback matter,
- (iii) Orientation effects that reduce the angular momentum perpendicular to the spin direction for a given transverse (i.e., non-radial) angular momentum of fallback matter,

³ The freefall timescale corresponding to this radius.

(iv) Feedback mechanisms in the vicinity of the neutron star that selectively limit accretion of angular momentum transverse to the kick direction.

It seems unlikely that uncertainties in the transverse angular momentum fluctuations prior to fallback could result in significantly lower specific angular momentum than suggested by Equation (13). Especially for typical pulsar magnetic field strengths well below the magnetar regime, transverse convective velocities correspond to a specific angular momentum somewhat above the critical value already. Fallback material could, of course, stem from regions that are initially non-convective, but given that a substantial fraction of supernova progenitors is taken up by convective shells, there would need to be a dynamical mechanism that facilitates fallback from non-convective regions in the progenitor. More importantly, even for spherically symmetric progenitor models long-time 3D supernova simulations (Chan et al. 2020; Janka et al. 2022) show quite robustly that hydrodynamic instabilities that act during the explosion⁴ generate sufficient transverse velocities for the specific angular momentum in fallback matter well above $10^{16} \text{ cm}^2 \text{ s}^{-1}$, i.e., sufficiently large for disk formation and even for staying outside the Alfvén radius. Thus, one expects that the distribution of specific angular momentum of accreted fallback material should extend up to the maximum allowed value and is not skewed towards zero within that range.

It also appears unlikely that variations in the transverse specific angular momentum of fallback matter average out effectively. Numerical simulation (Chan et al. 2020) show at most a few phases of spin-up and spin-down even for cases with high fallback masses, indicating that the accreted (vectorial) specific angular momentum is relatively stable and correlated over long time scales. The 3D simulations of Janka et al. (2022) also appear compatible with long correlation times in \mathbf{j} . At least for small fallback masses of no more than a few $0.01M_{\odot}$, one actually intuitively expects that spin-up by fallback should be determined by only a few spin-up phases with correlated angular momentum. The typical asymmetric structures emerging from the oxygen shell and shell further out during the explosion have low to medium wavenumbers ℓ (both because wide convective shells favour large-scale seed structures and because large-scale asymmetries develop generically during the engine phase), and the number of coherent plume structures within a shell will not be excessively high. Even if the fallback material stems from several such plume structures, stochastic cancellations of fallback material from different plumes should not be highly efficient, and the average specific angular momentum of accreted matter will not be reduced by orders of magnitude. Especially for material from the convective hydrogen envelope, where the specific angular momentum in convective seed motion is extremely large, it is therefore improbable that the average specific angular momentum of fallback material can be brought significantly below the critical value at the Alfvén radius.

Orientation effects imply that the accreted angular momentum generally has components both parallel and perpendicular to the kick direction. Janka et al. (2022) demonstrates that the neutron star should accrete from a cone with a half-angle of about $\pi/3$. If, as we have argued, the angular momentum of the fallback material is mostly perpendicular to its initial radius vector, the accreted angular momentum perpendicular to the kick should exceed a fraction of $\cot \pi/3 = 0.58$ of the component parallel to the kick, but will usually

be higher unless some feedback mechanism operating in the vicinity of the neutron star favours accretion of material parallel to the kick (see below). Thus, orientation effects cannot substantially reduce the transverse component of the angular momentum of fallback material either.

Finally, there might be some mechanism that inhibits the accretion of angular momentum perpendicular to the kick direction. This, however, could at best limit accretion to material from near the surface of the accretion cone, i.e., to material that still has considerable angular momentum transverse to the cone as we just discussed. There is no way to simply get rid of this angular momentum component completely once fallback material is approaching the neutron star. It can only be deposited on the neutron star or transferred to other fallback material in the vicinity of the neutron star by some mechanism that separates angular momentum perpendicular and transverse to the kick and then be ejected. However, one should naturally expect that outflows powered by the interaction of neutron stars with accreting matter should extract angular momentum from the neutron star, i.e., eject material with specific angular momentum aligned to the neutron star, and hence spin it down (cp. the case of propeller accretion, Alpar 2001; Romanova et al. 2004; Piro & Ott 2011). A mechanism that preferentially powers outflows that carry angular momentum transverse to that of the neutron star may not be impossible, but at present we view this as an unlikely possibility.

Incidentally, misalignment by fallback can, of course, be avoided if the neutron star *is* in the propeller regime and material gains angular momentum and energy by the interaction with the magnetosphere. For estimating limits on the accreted mass compatible with spin-kick alignment, ejection of fallback material in the propeller regime makes little difference. The possibility that fallback accretion may sometimes proceed in the propeller regime (Piro & Ott 2011) does not change the fact that any material that manages to be accreted will add to the neutron star the angular momentum it had prior to interaction with the magnetosphere; hence bounds on the amount of actually accreted material can still be deduced from the condition of limited spin-kick misalignment. It is just that the propeller regime may provide a *physical* mechanism for limiting the amount of accretion even if considerable fallback occurs. However, for large fallback masses, sufficiently early fallback times, and moderately strong neutron star magnetic fields, the propeller regime is avoided and matter that reaches the Alfvén radius with Keplerian velocity can be accreted. For the aforementioned example of $0.006M_{\odot}$ of fallback onto the Crab pulsar on a time scale of a 1 d, the Keplerian specific angular momentum at the Alfvén radius is about $3.6 \times 10^{16} \text{ cm}^2 \text{ s}^{-1}$, whereas the angular momentum for corotation at the Alfvén radius, $j_c = 2\pi P^{-1} R_A^2$, is only $2.3 \times 10^{15} \text{ cm}^2 \text{ s}^{-1}$. Thus, for moderately strong neutron star birth magnetic fields, the total amount of material that reaches the Alfvén radius in the first place likely has to be limited by the explosion physics to avoid spin-kick misalignment. The propeller mechanism could not stop substantial fallback onto the magnetosphere in such cases, though it may be relevant for limiting accretion at later stages or for stronger neutron star magnetic fields (Piro & Ott 2011).

As far as we can see, only one possible loophole for avoiding spin misalignment in the case of substantial fallback remains. If the kick is *initially* aligned with the rotation axis of the progenitor star, and if rotation is so fast as to push the pre-collapse convection zones into the limit of low Rossby number (where the rotational velocity exceed the convective velocity), the accreted angular momentum transverse to the kick direction would become negligible. As Janka et al. (2022) pointed out, however, this scenario is unlikely in the light of current simulation results that do not show spin-kick alignment even in the

⁴ This covers both neutrino-driven convection and the standing accretion shock instability during the pre-explosion or early explosion phase that imprint asymmetries on the ejecta initially, as well as mixing instabilities during the propagation of the shock through the envelope.

case of rapidly rotating progenitor models (Powell & Müller 2020; Powell et al. 2023). As long as the initial kick direction is selected randomly, one-sided accretion will tend to produce spin-kick misalignment in the case of rapid progenitor rotation (Janka et al. 2022). Thus, rotation is not likely to alter the findings outlined above. If rotation is fast (with rotation velocities exceeding pre-collapse convective velocities in a particular region), it will at most exacerbate the misalignment because stochastic cancellation of the angular momentum of accreted vortices should become less relevant.

All of these considerations suggest that the specific angular momentum perpendicular to the kick velocity of fallback material is probably only a factor of a few below our analytic estimates. The estimates from Equations (14,15) can therefore indeed be translated into upper limits for the amount of fallback in the formation of typical pulsars. Late-time fallback of not much more than $\sim 10^{-2} M_{\odot}$ on timescales of a day or more can be tolerated to maintain spin-kick alignment, and perhaps a bit more early on during the explosion. If a neutron star is born with a significantly longer period than 20 ms and shows spin-kick alignment, the limit on the amount of fallback accretion becomes more restrictive. Interestingly, the fallback masses of a few $10^{-3} M_{\odot}$ predicted by the 1D simulations of Ertl et al. (2016) for single stars and by Ertl et al. (2020) for stripped stars with final helium core masses below $\sim 6 M_{\odot}$ are consistent with this constraint. On the other hand, Ertl et al. (2020) predict substantial fallback of $\sim 0.1 M_{\odot}$ for some explosions for massive stripped stars in an island of explosibility with final helium core masses of $\gtrsim 10 M_{\odot}$. For these, the angular momentum imparted by fallback accretion should be substantial, in line with purely hydrodynamic long-time simulations of fallback in 3D by Chan et al. (2020). However, it seems premature to conclude that these explosions of high-mass progenitors should make a sub-population of neutron stars without spin-kick alignment. If a spin-kick alignment mechanism operates early on in these explosions during the “engine phase”, the initial angular momentum of the neutron star before fallback should be unusually high, as it will undergo substantial accretion and strong spin-up during the “engine phase” so that spin-tilting requires higher fallback masses. Moreover, only a small fraction of the neutron star population is expected to be affected by such high amounts of fallback.

5 CONCLUSION

Prompted by recent work of Janka et al. (2022) that highlighted the potential impact of one-sided fallback accretion on neutron star birth spins, we further analysed the expected angular momentum carried by vortices in shocked stellar material that may undergo fallback. We argue that one-sided accretion onto moving neutron stars will lead to spin-kick misalignment rather than alignment. Both pre-collapse convective motions and Rayleigh-Taylor instability during the supernova explosion predominantly create eddies with vorticity and angular momentum perpendicular to the radial direction. Accretion of material located in an accretion cone around the neutron star kick direction will therefore mostly add angular momentum perpendicular to the kick direction. Flattening of eddies by shock compression does not eliminate the transverse angular momentum components. Despite strong strong radial compression, the vorticity and angular momentum of pre-collapse convective eddies remain predominantly non-radial after being run over by the shock, even if the eddies are somewhat deformed and waves may somewhat redistribute angular momentum behind the shock front.

The realisation that fallback will more likely destroy rather than induce spin-kick alignment has implications both for the spin-kick

alignment mechanism and for fallback in core-collapse supernovae. First, the observed spin-kick alignment obviously still remains unexplained. If the mechanism involves (magneto-)hydrodynamic torques by accretion downflows, it likely has to operate early on during the explosion. Second, the tendency of fallback to misalign neutron star spins and kicks suggests limits on the typical amount of fallback that can be tolerated in supernova explosions.

In estimating spin-kick misalignment from fallback, one needs to take into account that accreted material has to come within about the Alfvén radius of the neutron star to effectively deposit its angular momentum. Based on this notion, we derived scaling laws for the maximum specific and total angular momentum of fallback (Equations 13–15). Estimates of the angular momentum contained in pre-collapse convective eddies as well as 3D simulations of fallback (Chan et al. 2020; Janka et al. 2022) suggest that the accreted material easily reaches or exceeds the Keplerian angular momentum at the Alfvén radius for typical neutron star birth magnetic field strengths, and that stochastic variations in the angular momentum direction of accreted matter should not push the estimates from Equations (13–15) down substantially. Equations (13–15) imply that young neutron stars should not accrete more than $\sim 10^{-2} M_{\odot}$ by fallback during the first day(s) of an explosion; otherwise the accreted angular momentum would be sufficient to misalign a neutron star with a spin period of 20 ms. For neutron stars with longer birth periods, the limit becomes more stringent. Pre-collapse rotation is not likely to weaken these upper bounds. The fallback masses currently predicted by parameterised 1D supernova explosion models (Ertl et al. 2016, 2020) are essentially compatible with these limits.

It is of course desirable to put the analytic estimates for neutron star spin-up and spin-kick misalignment by fallback on a firmer footing with the help of multi-dimensional simulations. The work by Janka et al. (2022) and our current study highlight, however, that there are non-trivial requirements for correctly tracking spin-up by fallback in such simulations. The motion of the neutron star, the three-dimensional structure of *all* the convective shells in the progenitor, and the coupling of fallback accretion streams with the neutron star magnetosphere may all turn out to be relevant. Whether a rigorous treatment of all of these effects in simulations is possible and can add yet another twist to the problem of spin-kick alignment remains to be seen.

ACKNOWLEDGEMENTS

I acknowledge helpful discussions with I. Mandel. This work was supported by ARC Future Fellowship FT160100035 and by the Australian Research Council (ARC) Centre of Excellence (CoE) for Gravitational Wave Discovery (OzGrav) project number CE170100004.

DATA AVAILABILITY

The data from our simulations will be made available upon reasonable requests made to the author.

REFERENCES

- Abdikamalov E., Foglizzo T., 2020, *MNRAS*, 493, 3496
- Abdikamalov E., Zhakyslykov A., Radice D., Berdibek S., 2016, *MNRAS*, 461, 3864
- Alpar M. A., 2001, *ApJ*, 554, 1245
- Antoni A., Quataert E., 2022, *MNRAS*, 511, 176

- Antoni A., Quataert E., 2023, *MNRAS*,
- Arras P., Lai D., 1999, *ApJ*, 519, 745
- Barbosa F. J., Skews B. W., 2001, *Physics of Fluids*, 13, 3049
- Biermann L., 1932, *Z. Astrophys.*, 5, 117
- Blondin J. M., Mezzacappa A., DeMarino C., 2003, *ApJ*, 584, 971
- Böhm-Vitense E., 1958, *Z. Astrophys.*, 46, 108
- Bollig R., Yadav N., Kresse D., Janka H.-T., Müller B., Heger A., 2021, *ApJ*, 915, 28
- Burrows A., Vartanyan D., 2021, *Nature*, 589, 29
- Burrows A., Hayes J., Fryxell B. A., 1995, *ApJ*, 450, 830
- Chan C., Müller B., Heger A., Pakmor R., Springel V., 2018, *ApJ*, 852, L19
- Chan C., Müller B., Heger A., 2020, *MNRAS*, 495, 3751
- Chevalier R. A., 1976, *ApJ*, 207, 872
- Cognard I., Shrauner J. A., Taylor J. H., Thorsett S. E., 1996, *ApJ*, 457, L81
- Coleman M. S. B., Burrows A., 2022, *MNRAS*, 517, 3938
- Ebinger K., Curtis S., Fröhlich C., Hempel M., Perego A., Liebendörfer M., Thielemann F.-K., 2019, *ApJ*, 870, 1
- Einfeldt B., 1988, *SIAM Journal on Numerical Analysis*, 25, 294
- Ellzey J. L., Henneke M. R., Picone J. M., Oran E. S., 1995, *Physics of Fluids*, 7, 172
- Ertl T., Ugliano M., Janka H.-T., Marek A., Arcones A., 2016, *ApJ*, 821, 69
- Ertl T., Woosley S. E., Sukhbold T., Janka H. T., 2020, *ApJ*, 890, 51
- Fragione G., Loeb A., 2023, Neutron star kicks and implications for their rotation at birth ([arXiv:2305.08920](https://arxiv.org/abs/2305.08920)), doi:10.48550/arXiv.2305.08920
- Fryxell B., Arnett D., Mueller E., 1991, *ApJ*, 367, 619
- Fuller J., Piro A. L., Jermyn A. S., 2019, *MNRAS*, 485, 3661
- Gilkis A., Soker N., 2014, *MNRAS*, 439, 4011
- Gresho P. M., Chan S. T., 1990, *International Journal for Numerical Methods in Fluids*, 11, 621
- Harrison E. R., Tademaru E., 1975, *ApJ*, 201, 447
- Heger A., Langer N., Woosley S. E., 2000, *ApJ*, 528, 368
- Heger A., Woosley S. E., Spruit H. C., 2005, *ApJ*, 626, 350
- Herant M., Benz W., Colgate S., 1992, *ApJ*, 395, 642
- Herant M., Benz W., Hix W. R., Fryer C. L., Colgate S. A., 1994, *ApJ*, 435, 339
- Huete C., Abdikamalov E., Radice D., 2018, *MNRAS*, 475, 3305
- Igoshev A. P., Popov S. B., 2013, *MNRAS*, 432, 967
- Illarionov A. F., Sunyaev R. A., 1975, *A&A*, 39, 185
- Janka H.-T., 2013, *MNRAS*, 434, 1355
- Janka H.-T., Müller E., 1995, *ApJ*, 448, L109
- Janka H.-T., Müller E., 1996, *A&A*, 306, 167
- Janka H.-T., Wongwathanarat A., Kramer M., 2022, *ApJ*, 926, 9
- Johnston S., Hobbs G., Vigeland S., Kramer M., Weisberg J. M., Lyne A. G., 2005, *MNRAS*, 364, 1397
- Kifonidis K., Plewa T., Scheck L., Janka H.-T., Müller E., 2006, *A&A*, 453, 661
- Kou F. F., Tong H., 2015, *MNRAS*, 450, 1990
- Kovalenko I. G., Eremin M. A., 1998, *MNRAS*, 298, 861
- Kramer M., Lyne A. G., Hobbs G., Löhmer O., Carr P., Jordan C., Wolszczan A., 2003, *ApJ*, 593, L31
- Lai D., Goldreich P., 2000, *ApJ*, 535, 402
- Lai D., Chernoff D. F., Cordes J. M., 2001, *ApJ*, 549, 1111
- Langer N., 2012, *ARA&A*, 50, 107
- Lyne A. G., Jordan C. A., Graham-Smith F., Espinoza C. M., Stappers B. W., Weltevrede P., 2015, *MNRAS*, 446, 857
- Lyutikov M., 2007, *MNRAS*, 381, 1190
- Müller B., 2020, *Living Rev. Comput. Astrophys.*, 6, 3
- Müller E., Fryxell B., Arnett D., 1991, *A&A*, 251, 505
- Müller B., Heger A., Liptai D., Cameron J. B., 2016a, *MNRAS*, 460, 742
- Müller B., Viallet M., Heger A., Janka H.-T., 2016b, *ApJ*, 833, 124
- Müller B., Melson T., Heger A., Janka H.-T., 2017, *MNRAS*, 472, 491
- Müller B., et al., 2019, *MNRAS*, 484, 3307
- Noutsos A., Kramer M., Carr P., Johnston S., 2012, *MNRAS*, 423, 2736
- Noutsos A., Schnitzeler D. H. F. M., Keane E. F., Kramer M., Johnston S., 2013, *MNRAS*, 430, 2281
- Piro A. L., Ott C. D., 2011, *ApJ*, 736, 108
- Popov S. B., Turolla R., 2012, *Ap&SS*, 341, 457
- Powell J., Müller B., 2019, *MNRAS*, 487, 1178
- Powell J., Müller B., 2020, *MNRAS*, 494, 4665
- Powell J., Müller B., Aguilera-Dena D. R., Langer N., 2023, *MNRAS*, 522, 6070
- Quirk J. J., 1994, *International Journal for Numerical Methods in Fluids*, 18, 555
- Richtmyer R. D., 1960, *Communications on Pure and Applied Mathematics*, 13, 297
- Romanova M. M., Ustyugova G. V., Koldoba A. V., Lovelace R. V. E., 2004, *ApJ*, 616, L151
- Scheck L., Kifonidis K., Janka H.-T., Müller E., 2006, *A&A*, 457, 963
- Shapiro S. L., Teukolsky S. A., 1983, *Black Holes, White Dwarfs, and Neutron Stars: The Physics of Compact Objects*. Wiley-Interscience, New York
- Socrates A., Blaes O., Hungerford A., Fryer C. L., 2005, *ApJ*, 632, 531
- Soker N., 2023, *MNRAS*, 520, 4404
- Spruit H., Phinney E. S., 1998, *Nature*, 393, 139
- Stockinger G., et al., 2020, *MNRAS*, 496, 2039
- Sukhbold T., Ertl T., Woosley S. E., Brown J. M., Janka H.-T., 2016, *ApJ*, 821, 38
- Toro E. F., Spruce M., Speares W., 1994, *Shock Waves*, 4, 25
- Ugliano M., Janka H.-T., Marek A., Arcones A., 2012, *ApJ*, 757, 69
- Velikovich A. L., Wouchuk J. G., Huete Ruiz de Lira C., Metzler N., Zalesak S., Schmitt A. J., 2007, *Physics of Plasmas*, 14, 072706
- Wang C., Lai D., Han J. L., 2007, *ApJ*, 656, 399
- Wongwathanarat A., Janka H., Müller E., 2010, *ApJ*, 725, L106
- Wongwathanarat A., Janka H.-T., Müller E., 2013, *A&A*, 552, A126
- Wongwathanarat A., Müller E., Janka H.-T., 2015, *A&A*, 577, A48
- Wouchuk J. G., Huete Ruiz de Lira C., Velikovich A. L., 2009, *Phys. Rev. E*, 79, 066315
- Yao J., et al., 2021, *Nature Astronomy*, 5, 788
- Zhang S., Zhang Y.-T., Shu C.-W., 2005, *Physics of Fluids*, 17, 116101
- Zhou Y., 2017a, *Phys. Rep.*, 720, 1
- Zhou Y., 2017b, *Phys. Rep.*, 723, 1
- van Leer B., 1974, *Journal of Computational Physics*, 14, 361

This paper has been typeset from a $\text{\TeX}/\text{\LaTeX}$ file prepared by the author.